Desalination and Water Treatment
www.deswater.com
doi: 10.1080/19443994.2015.1058728

57 (2016) 13586–13599
June

Taylor & Francis
Taylor & Francis Group

A Plug flow reactor model for UV-based oxidation of amoxicillin

Sifa Dogan*, Rana Kidak

Faculty of Engineering, Department of Environmental Engineering, Cyprus International University, Mersin 10, Turkey, Tel. +90 0392 671 11 11/2345; email: sdogan@ciu.edu.tr (S. Dogan), Tel. +90 0392 671 11 11/2409; email: rkidak@ciu.edu.tr (R. Kidak)

Received 29 March 2015; Accepted 1 June 2015

ABSTRACT

Amoxicillin was treated with UV and UV/H_2O_2 processes, and the byproduct formation, mineralization and toxicity on *Vibrio fischeri* (a luminescent micro-organism) were monitored to satisfy environmental considerations. A plug flow cylindrical reactor (33 cm length and 1.75 cm radius) and a peristaltic pump (multifunctional speed pump) were used to perform the treatments. A UV lamp covered with a quartz protection was placed inside the reactor. The UV fluence rate was calculated with a chemical actinometry method, and its value was 2.3 W m^{-2}. The maximum removal of amoxicillin with the UV and UV/H_2O_2 processes was achieved when the peristaltic pump speed was adjusted to 10 rpm and the H_2O_2 concentration to 588 mg L^{-1} (55 and 90%, respectively). In addition, under the above-mentioned optimal conditions, the mineralization was 11 and 43% for the UV and UV/H_2O_2 processes, respectively. A byproduct formation pathway was proposed for each process. When the flow reactor was operated in the presence of alkalinity (20.5 mg $CaCO_3$ L^{-1}) and humic acid (5 mg L^{-1}), a 50% decrease in the removal performance was observed due to the applied matrix parameters. The EC_{50}% value was 76 and 36% after the UV and UV/H_2O_2 treatments, which indicates the toxicity level of the effluents after 67 min of UV-based oxidation treatments.

Keywords: Pharmaceutical pollution; Water pollution; Amoxicillin; Advanced oxidation; UV irradiation; UV/H_2O_2 process; Byproduct formation; Toxicity; EC_{50}%

1. Introduction

Water resources are contaminated with pharmaceutical waste due to the increased use of drugs for treating various human and animal diseases. Recently, the WHO reported the severe effects caused by pharmaceutically active compounds in aquatic environments, natural habitats and living organisms. These detrimental effects include the generation of antibiotic-resistant micro-organisms, aquatic toxicity, genotoxicity, and endocrine disruptions [1–4]. Among these pharmaceutical products, amoxicillin is one of the most frequently prescribed antibiotics used to treat a broad spectrum of Gram (−) and Gram (+) bacterial diseases [5]. After the intake of amoxicillin, 60% is excreted and thus enters the municipal or hospital wastewaters. Inefficient treatment techniques result in a discharge of treated effluents that contain concentrations ranging from ng/L to μg/L levels of antibiotics [6–9]. Conventional treatment techniques are not able to remove such antibiotics because of their high water solubility (3.4 g/L) and resistance to biodegradation [10]. Advanced oxidation processes (AOPs) are the only treatment alternatives to eliminate such

*Corresponding author.

1944-3994/1944-3986 © 2015 Balaban Desalination Publications. All rights reserved.

antibiotics from the wastewater effluents and induce their mineralization [11].

AOPs produce $OH^{\cdot}$ radicals by chemical, photochemical, photocatalytic, or electrochemical reactions that hydroxylate organic compounds until they are completely mineralized [12]. The most frequently preferred AOP techniques are UV photolysis, ozonation, and Fenton's method, which includes UV/H_2O_2, UV/O_3, $UV/H_2O_2/O_3$, $UV/O_3/Fe^{2+}$, H_2O_2/Fe^{2+}, and $UV/H_2O_2/Fe^{2+}$ [12,13]. Among those processes, the treatments with UV and UV/H_2O_2 are the most widely applied in large scale and laboratory research applications. Several authors have reported a percentage of amoxicillin removal >99% in aqueous solutions using Fenton's process [14–23]. However, the resulting sludge production is the major drawback of Fenton's process after iron molecules are added to the system.

Ozonation and catalytic ozonation are also powerful techniques to totally eliminate amoxicillin molecules within short reaction times. However, the *in situ* production and dissolution of short-lived O_3 molecules are occasionally difficult to handle [24–26].

Therefore, the process of UV irradiation constitutes a compatible option for the treatment of non-biodegradable compounds such as antibiotics. Hence, the investigation of the overall process is crucial. The UV-based advanced oxidation techniques promise high degradation rates of amoxicillin. For instance, 100 μg/L–100 mg/L of aqueous amoxicillin was completely eliminated within 30–60 min by UV/H_2O_2, UV/TiO_2, $UV/H_2O_2/TiO_2$, and UV/ZnO processes under several UV doses. For further mineralization, it was necessary to extend the reaction time to achieve 50% TOC removal and 20–50% COD removal [26–29]. Several studies have proposed possible degradation pathways [30,31].

To this date, no study has been performed to assess the removal efficiency of amoxicillin in a plug flow reactor system. Likewise, the byproduct profile and toxicity level have not been evaluated in this system. In this study, the effects of matrix parameters such as humic acids as a model of natural organic matter (NOM) and alkalinity, which are the major background components of wastewaters were measured. The literature only provides studies performed for the purpose of investigating the process efficiency with spiked real water samples and amoxicillin as the target molecule [32,33]. This study focuses on the evaluation of UV and UV/H_2O_2 processes by combining several aspects in addition to the treatment efficiency. Moreover, the applicability of the plug flow reactor was tested with the UV and UV/H_2O_2 processes for the treatment of large volumes of wastewaters.

2. Materials and methods

2.1. Chemicals

Amoxicillin (Sigma-Aldrich Potency 900 μg, CAS No: 26787-78-0), potassium peroxodisulfate (for analysis, Merck, CAS No: 7727-21-1) tert-butanol (Merck, CAS No: 75-65-0), and acetonitrile (Gradient grade for LC, LICHROSOLV, CAS No: 75–05-8) were purchased from the Isomer Laboratory and Medical Supplies Ltd, Cyprus. Distilled water was obtained from Sartorius 61316, and a 611 UV ultrapure water system was purchased from Sartonet, Turkey. Sodium bicarbonate (for analysis, Merck, CAS No: 144-55-8), humic acid disodium salt (Sigma Aldrich, CAS No: 68131-04-4), hydrogen peroxide (35%, Merck, CAS No: 7722-84-1), a cylindrical glass reactor, a UV lamp (Lighttech, low-pressure mercury-arc germicidal lamp, UV Output 254 nm, Power 21 W), and a peristaltic pump (multifunctional pump speed, Behr-Labor-Technik) were obtained from Tin Chemical and Laboratory Supplies and Devices, Turkey. C_{18} cartridges (Finisterre by Teknokroma, SPE C18 100 mg/6 mL) were purchased from ENOTEK, Turkey. A *Vibrio fischeri* reagent (SDI, Strategic Diagnostics Inc., Part No: AZF686018A), a diluent (SDI, Strategic Diagnostics Inc., Part No: AZF686011), a reconstitution solution (SDI, Strategic Diagnostics Inc., Part No: AZF686016), and an osmotic adjusting solution (SDI, Strategic Diagnostics Inc., Part No: AZF686019) were obtained from KEMITEKS Polymer Emulsions & Pigment Dispersions Company, Turkey.

2.2. Analytical techniques

A high-performance liquid chromatography (HPLC) coupled with a UV–vis detector (Shimadzu, 2010) was used for the detection of aqueous amoxicillin molecules at a 204 nm wavelength. A 50 × 2.00 mm Synergi 4 μ Fusion RP 80A analytical column was used as a stationary phase, and a mobile phase was prepared with a 99:1 ratio of water:acetonitrile. The flow rate was kept at 1 mL/min, the injection volume was adjusted to 10 μL, and the oven temperature was kept at 40°C. The limit of detection was 0.25 mg L^{-1}.

The humic acid concentration was calculated by measuring the absorbance values at 254 nm through a Schimadzu UV-2450 UV–vis spectrophotometer. The interference resulting from the presence of humic acid in the measurement of amoxicillin concentration was avoided by a chromatographic elution with the HPLC method.

The UV photon flux was calculated by the chemical actinometry method described in the literature [34], and it was 4.86×10^{-6} Einstein m^{-2} s^{-1} (2.3 W m^{-2}).

The byproduct identification was performed by monitoring the mass spectrum of each peak observed after the UV and UV/H_2O_2 treatment of amoxicillin with a gas chromatograph–mass spectrophotometer (GCMS; Schimadzu, GCMS 2010 Plus). Prior to the GCMS analysis, all the samples were extracted into an organic phase. The solid phase extraction procedure was performed with 5 mL of methanol for conditioning the C_{18} cartridges. Then, 50 mL of treated samples was passed through the cartridges, and the elution was made with 5 mL of methanol. Finally, 5 mL of distilled water was used to wash up the cartridges. A GCMS analysis was carried out on a TRB-5MS (length 30 m, ID 20 mm, with a 0.25 μm film coating) capillary column and directly injected to the ion source by a transfer line heated to 250°C. The chromatographic separation was performed with an initial temperature of 100°C for 2 min. Afterwards, the temperature rose at a rate of 15°C/min until it reached 150°C, and it remained constant for 5 min. An ion source tuning test was carried out prior to each GCMS analysis. The detector voltage was below 1.5 kV (0.83 kV). The repeatability test of the GCMS analysis was performed with octafluoronaphthalene (100 pg). The area repeatability and retention time repeatability was set at a % RSD < 5% and a % RSD < 1%, respectively. In addition, prior to the GCMS analysis, a PTFBA (perfluorotributylamine) analytical standard was used to correct the mass axis alignments.

The toxicity of treated effluents was calculated by testing the light intensity of *Vibrio fischeri* microorganisms with a Microtox SDI Model 500 spectrophotometer. The treated effluents were diluted to 50% four times and added into the micro-organism-containing solutions. The initial and final light intensities were recorded, and a logarithmic relationship was obtained by plotting light intensity vs. concentration. The effective concentration that disrupted the normal conditions of 50% of the population of *Vibrio fischeri* micro-organisms (EC_{50}%) was calculated with this relationship for the UV- and UV/H_2O_2-treated samples.

2.3. Experimental setup

The experiments were conducted in a cylindrical reactor with a total volume of 680 cm^3. A UV lamp was placed in the middle of the reactor and covered with a quartz tube. The water samples were transferred into the reactor by a peristaltic pump. The experimental setup is shown in Fig. 1.

The residence time for several pumping rates was calculated by dividing the total volume (cm^3) by the volumetric flow rate (cm^3/min). Several 25 mg L^{-1} aqueous solutions were treated in the reactor to observe the mineralization process, the byproduct formation and the toxicity of treated effluents by analytical methods under neutral pH conditions. The UV photolysis of the solutions was tested at several pumping rates (10, 20, 30, 40, 50, 60, and 90 rpm). The UV/H_2O_2 optimization was performed using three different H_2O_2 dosages (97, 194, and 588 mg L^{-1}). Aliquots were collected after the residence time, and

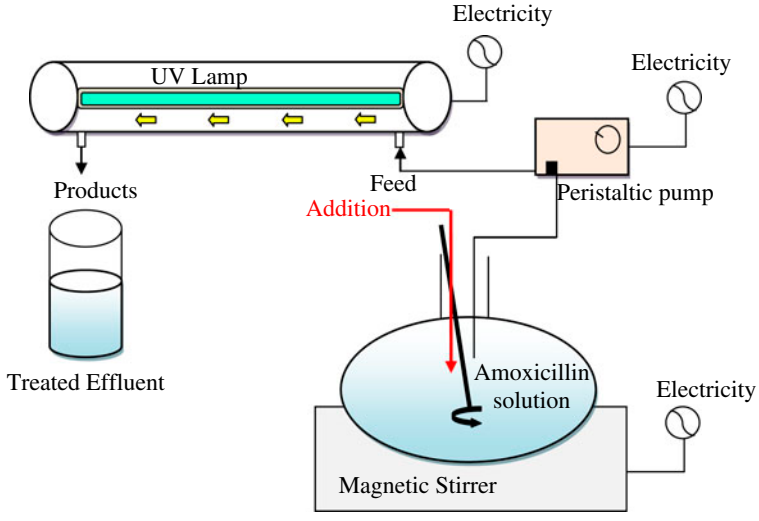

Fig. 1. Experimental setup.

Table 1
Reactor dimensions

Dimension	Value	Unit
Reactor length, l	33.0	cm
Radius of UV lamp, R_1	1.50	cm
Radius of quartz tube, R_2	1.75	cm
Radius of reactor, R_3	3.55	cm
Surface area of quartz tube[a], S_1	363	cm^2
Surface area of reactor[a], S_2	736	cm^2
Surface area of solution for irradiation[b], S	550	cm^2
Path length of UV irradiation[c]	1.80	cm
Total sample volume	680	cm^3

[a]Surface area of the cylinder $2 \times \pi \times$ diameter $\times$ length.
[b]S was calculated by $(S_1 + S_2)/2$. The maximum and minimum irradiation surfaces are S_1 and S_2: therefore, the irradiated surface area during the reaction was determined by the calculation of the average.
[c]UV irradiation was occurred from quartz tube to the surface of the reactor. Therefore, the path length was calculated by subtraction of R_2-R_3.

measurements of concentration, byproduct, mineralization, and toxicity were performed. The bicarbonate alkalinity of the experiments was set to 20.5 mg L^{-1} with $CaCO_3$. In natural water, the humic acid varies from 2 to 10 mg L^{-1} [35]. Therefore, 5 mg L^{-1} of humic acid was applied to the amoxicillin-containing aqueous solutions to test the effects of NOM on the amoxicillin removal by the UV and UV/H_2O_2 processes. Finally, the effects of both parameters were tested by the addition of sufficient amounts of humic acid and alkalinity into the aqueous solutions of amoxicillin.

Animal and Human Rights were preserved within all the experiments.

3. Results

3.1. Reactor model

The reactor length and width were selected according to the length of the UV lamp used. The dimensions of the flow reactor are given in Table 1 and illustrated in Fig. 2. With these dimensions, the total reactor volume was 680 cm^3.

The residence time for each pump speed (10, 20, 30, 40 50, 60, and 90 rpm) was calculated by dividing the total volume (cm^3) by the volumetric flow rate (cm^3/min). The results are given in Table 2.

The UV fluence rate was measured by the irradiation of a mixture of 0.01 M potassium peroxodisulfate and 0.1 M tert-butanol. The pH was recorded after each residence time, and the $[H^+]$ vs. residence time data were plotted. The slope of the linear line was 4×10^{-6}, and the incident fluence rate (I_o) was calculated using Eqs. (1) and (2), where Φ (H^+) is the quantum yield of H^+ formation (reference value 1.8); V_{tot} denotes the total sample volume (cm^3); M is the surface area of the irradiated solution (cm^2); the $[H^+]/t$ value (mol dm^{-3} s^{-1}) was obtained from the slope of $[H^+]$ vs. the t graph (4×10^{-6}); I_{abs}/N_L (N_L, Avogadro number) is the absorbed fluence rate in

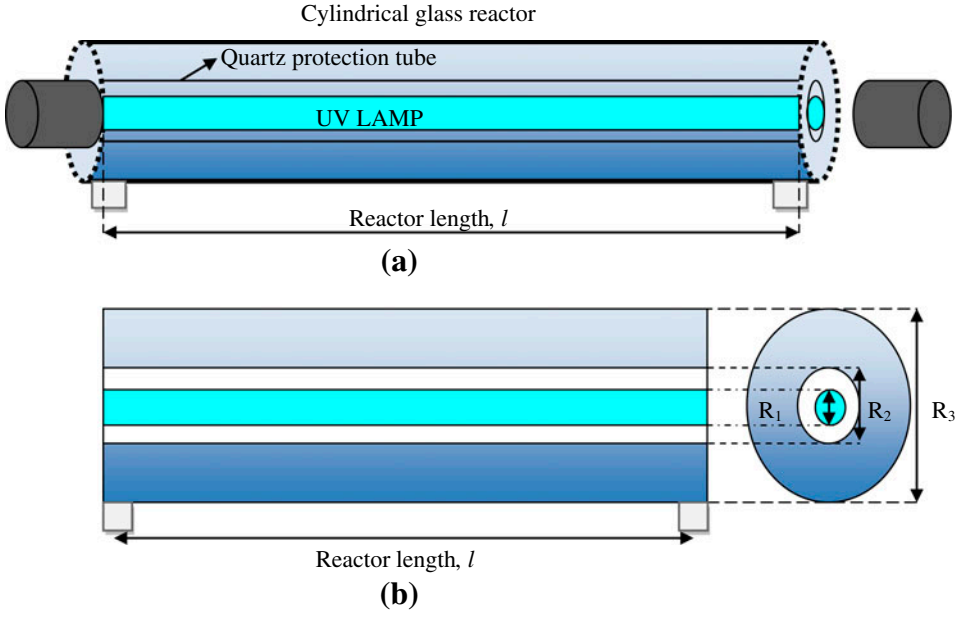

Fig. 2. (a) Front view of the plug flow reactor and (b) surface area dimensions of the reactor.

Table 2
Residence time calculation for each pump speed (total sample volume = 680 cm^3 and constant density assumption)

Pump speed (rpm)	Average flow rate (cm^3/min)	Residence time (min)
10	10.2	67.0
20	17.8	38.0
30	26.5	25.6
40	34.0	19.9
50	45.0	15.1
60	55.3	12.3
90	74.0	9.20

terms of Einsteins m^{-2} s^{-1}; I_{abs} is the absorbed photon fluence rate; I_o is the incident photon fluence rate; l is the path length; and ε and c are the molar extinction coefficient (20 dm^3 mol^{-1} cm^{-1}) and the concentration of potassium peroxodisulfate (0.01 M), respectively. I_o was calculated as 4.86×10^{-6} Einstein m^{-2} s^{-1} (2.3 W m^{-2}) [34].

$$\Phi\ (H^+) = \frac{[H]^+ \times N_L \times V_{tot} \times 10}{t \times I_{abs} \times M} \quad (1)$$

$$I_{abs} = I_o(1-10^{-\varepsilon.c.l}) \quad (2)$$

3.2. Removal of amoxicillin with UV and UV/H_2O_2

Seven different pump speeds were applied to test the removal efficiency of the UV irradiation to treat aqueous solutions with 25 mg L^{-1} amoxicillin. The maximum removal (55%) occurred when the system operated at 10 rpm. In addition, the mineralization measurement showed that 11% TOC was eliminated. When the system operated at pump speeds higher than 40 rpm, no removal was observed due to the short residence time.

To increase the removal of amoxicillin, a well-known oxidizing chemical, hydrogen peroxide (H_2O_2), was added to the UV system. The irradiation of UV light with H_2O_2 resulted in the production of hydroxyl radicals (OH·), which are capable of unselectively attacking several types of organic contaminants and causing their elimination. Three different concentrations of H_2O_2 (97, 194, and 588 mg L^{-1}) were tested to determine the optimum dosage. The highest removal (92%) occurred when the H_2O_2 concentration was adjusted to 588 mg L^{-1} with an optimal pump speed of 10 rpm and a residence time of 67 min. The mineralization increased up to 43% with the UV/H_2O_2 system. With the optimal dosage of H_2O_2, the UV/H_2O_2 process was applied at different pump speeds and above 50 rpm, no amoxicillin removal and mineralization was achieved. Detailed results are shown in Figs. 3 and 4.

Kinetic investigations were performed to compare the UV and UV/H_2O_2 processes. The remaining concentration (C/Co) vs. the residence time were plotted to reveal the curve of the degradation reaction. To investigate the kinetics of the UV/H_2O_2 process, 588 mg L^{-1} H_2O_2 was used. The degradation curves followed first-order kinetics (Fig. 5), and the observed first-order reaction rate constants for the UV and UV/H_2O_2 processes were 0.0119 and 0.0345 min^{-1}, respectively.

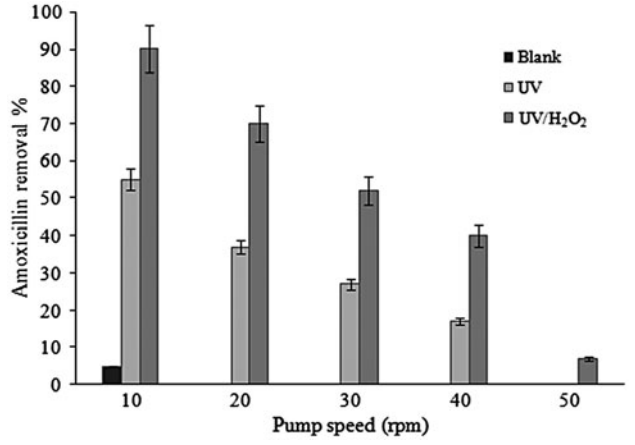

Fig. 3. Removal percentage of amoxicillin by UV and UV/H_2O_2 processes at various pump speeds (C = 25 mg L^{-1}, [H_2O_2] = 588 mg L^{-1}, and UV fluence rate = 4.86×10^{-6} Einstein m^{-2} s^{-1}).

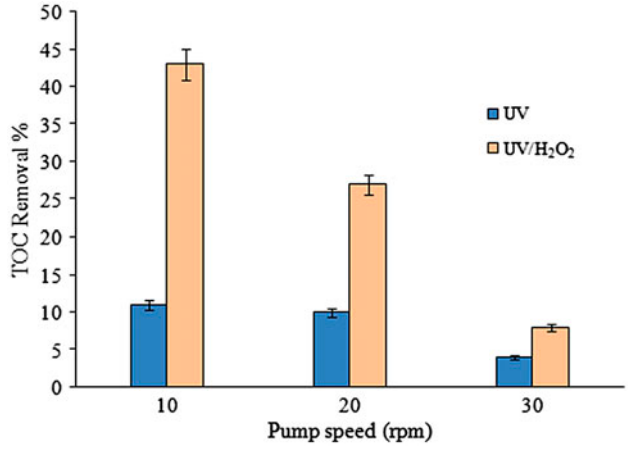

Fig. 4. TOC removal percentage of amoxicillin treatment by UV and UV/H_2O_2 at various pump speeds (C = 25 mg L^{-1}, [H_2O_2] = 588 mg L^{-1}, and UV fluence rate = 4.86×10^{-6} Einstein m^{-2} s^{-1}).

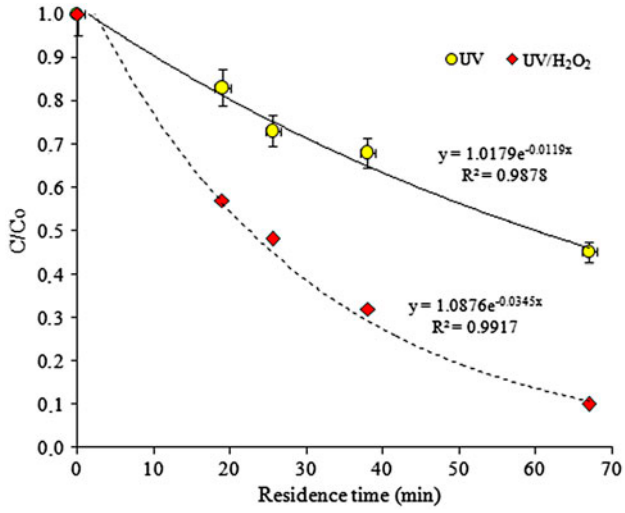

Fig. 5. Degradation curves of UV- and UV/H_2O_2-treated amoxicillin solutions (C = 25 mg L^{-1}, $[H_2O_2]$ = 588 mg L^{-1}, and UV fluence rate = 4.86×10^{-6} Einstein m^{-2} s^{-1}).

3.3. Process efficiency in the presence and absence of the effects of alkalinity and humic acid

The alkalinity in the water samples mostly arose as a consequence of the presence of bicarbonate (HCO_3^-) and carbonate ions (CO_3^{2-}) [36,37]. In the literature, the effect of alkalinity has been investigated by several authors, and it has been shown that alkalinity causes chemical species to react with OH· and act as a scavenger ($k_{CO_3^{2-}} = 3.7 \times 10^8$ M^{-1} s^{-1} and $k_{HCO_3^-} = 8 \times 10^6$ M^{-1} s^{-1}) [36,38,39]. In this study, the presence of bicarbonate ions severely affected the removal efficiency and resulted in only 13% (UV) and 23% (UV/H_2O_2) of amoxicillin removal and in 2% (UV) and 12% (UV/H_2O_2) of mineralization.

The excreta of humans and land animals contain soluble refractory organic matter that survives in the effluents of wastewater treatment plants. The UV irradiation and the radicals that are formed during the UV/H_2O_2 treatment process attack all the molecules, including the target molecule. Therefore, the treatment efficiency significantly decreases when humic acids, which represent the soluble refractory matter, are involved in the treatment parameters [40] because they consume the irradiation and/or the radicals produced. When humic acid was added, only 17% (UV) and 24% (UV/H_2O_2) of amoxicillin was removed, and 8% (UV) and 16% (UV/H_2O_2) of mineralization was obtained. The results showed that approximately 9% of humic acid was eliminated by both systems after 67 min of residence time.

The treatment efficiency decreased to 14% (UV) and 31% (UV/H_2O_2) when the amoxicillin solution contained both bicarbonate ions and humic acid. No mineralization was observed for the UV process, and only 12% mineralization was achieved by the UV/H_2O_2 process.

The performance of the amoxicillin removing system in the presence and absence of alkalinity and humic acid is shown in Fig. 6.

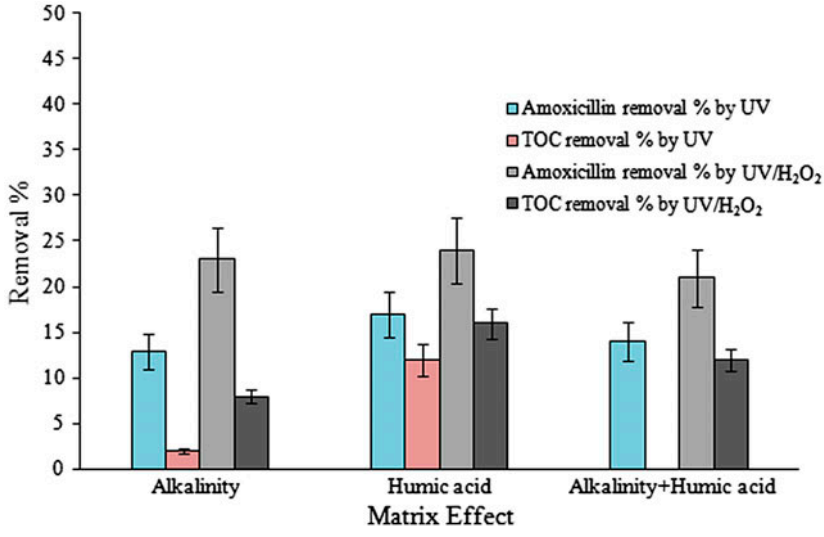

Fig. 6. System performance of removing amoxicillin molecules in the presence and absence of alkalinity and humic acid species (C = 25 mg L^{-1}, Bicarbonate alkalinity = 20.5 mg L^{-1}, Humic acid species = 5 mg L^{-1}, Pump speed = 10 rpm, $[H_2O_2]$ = 588 mg L^{-1}, and UV fluence rate = 4.86×10^{-6} Einstein m^{-2} s^{-1}).

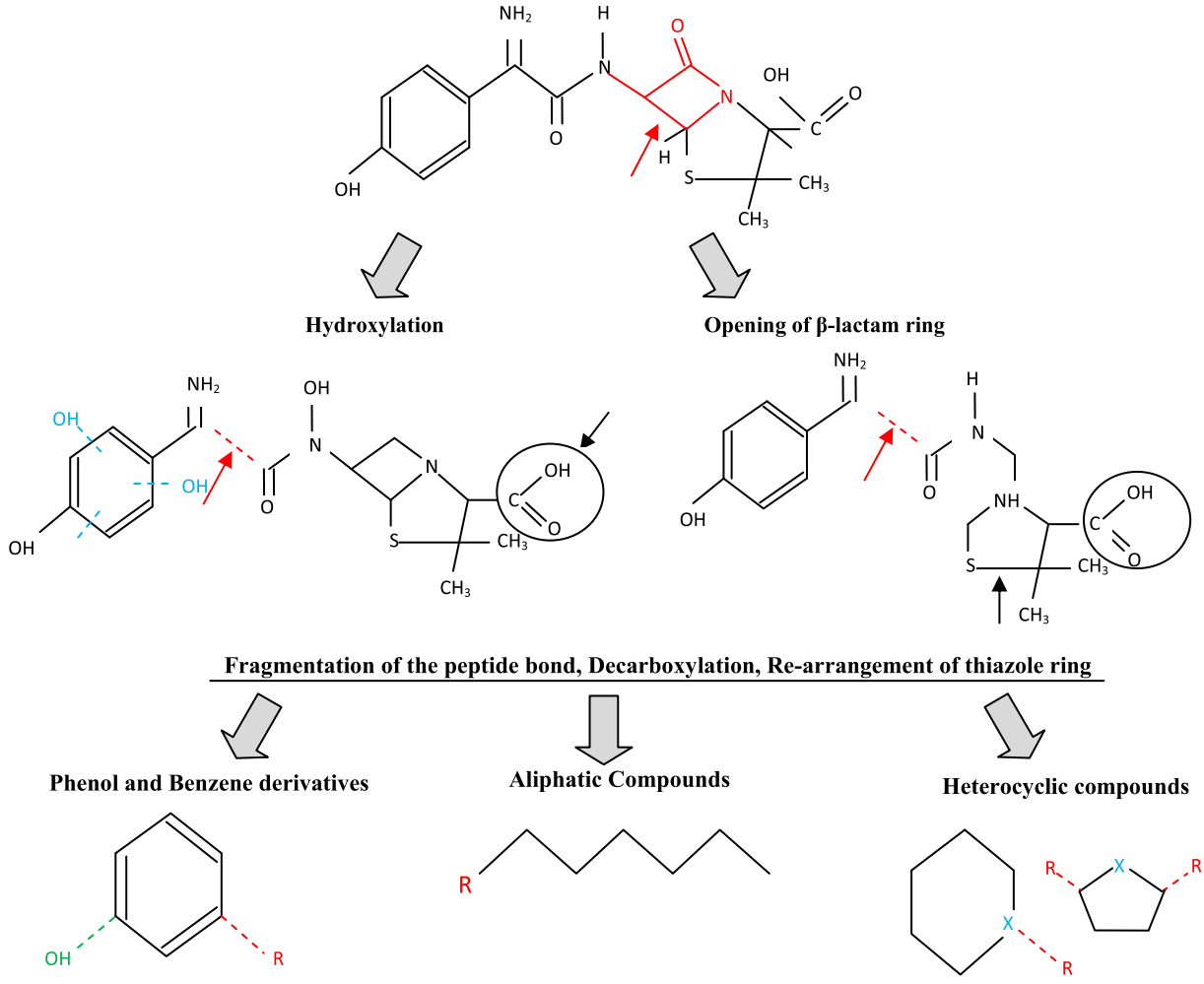

Fig. 7. Possible pathways of amoxicillin degradation.

3.4. Byproduct monitoring

Three possible oxidative degradation pathways (Fig. 7) have been proposed for the decomposition of amoxicillin in the literature [15,29,30,41]:

(1) Hydroxylation: addition of OH· to the parental compound.
(2) Opening of the four-membered β-lactam ring.
(3) Decarboxylation of free carboxylic acid and rearrangement of the five-membered thiazole ring.

The identification of the byproducts was performed by evaluating the mass spectrum of each compound to identify each molecule through its fragmentation.

The proposed degradation pathway of the UV and UV/H_2O_2 removal of amoxicillin is given in Figs. 8 and 9, and the fragmentation tables are illustrated in Table 3.

The proposed degradation pathway according to the identified byproducts of treated amoxicillin solutions with UV suggests that the irradiated amoxicillin molecules lose an oxygen atom (a) and a methyl group (demethylation). Initially, the opening of the thiazole ring (b) also occurs. This is followed by a decarboxylation process (loss of –COOH) and the loss of a sulfur atom. Moreover, a rearrangement occurs between the carbon, hydrogen, and oxygen elements (c and d). Finally, the mineralization of the solutions results in the loss of the aliphatic chain of the remaining molecules, and several pathways (e–g) follow to produce the identified byproducts. The degradation pathway with UV irradiation in the presence of humic acid followed a different pathway (a–d). Because the elimination of amoxicillin decreased with the addition

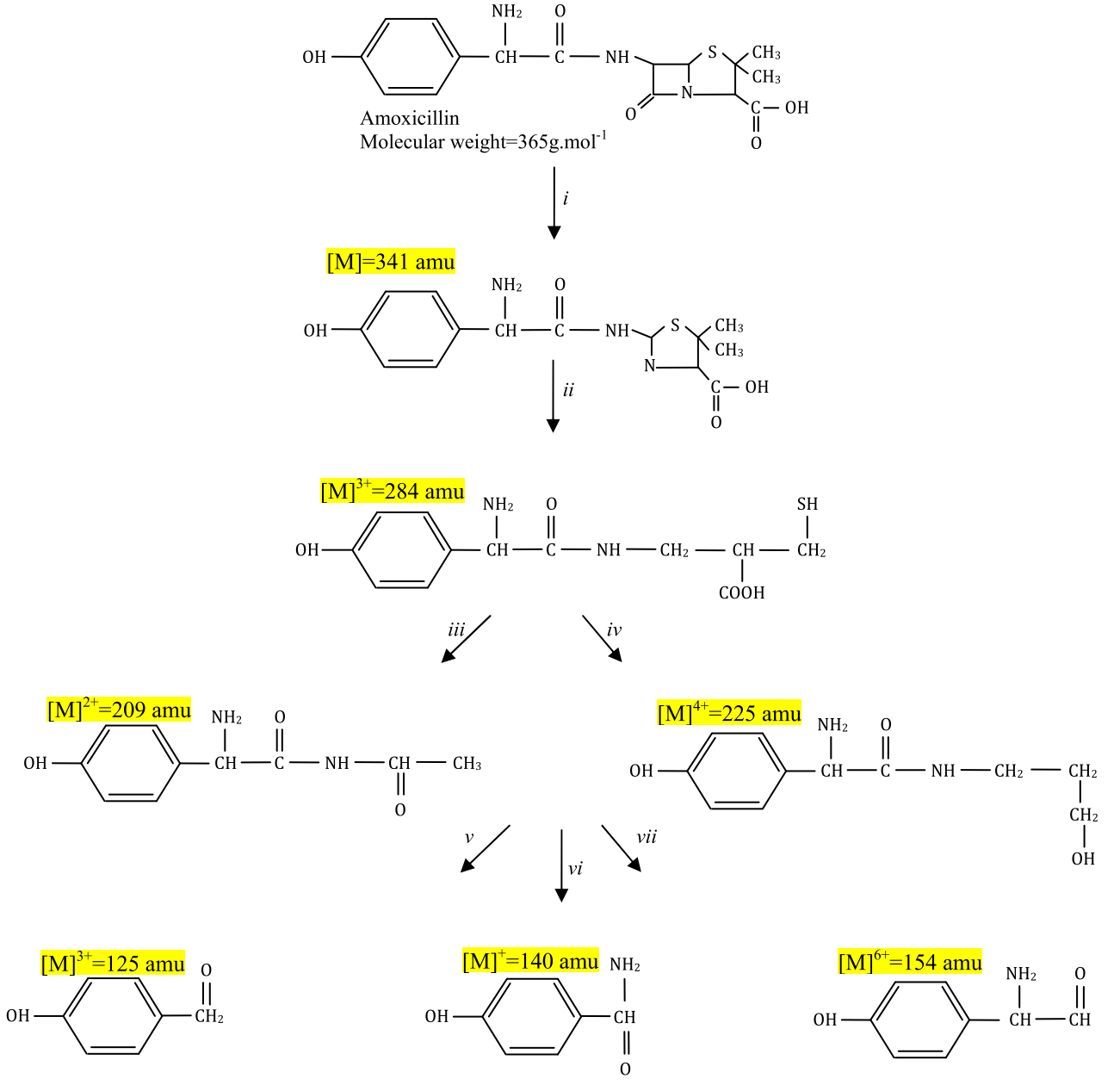

Fig. 8. Proposed degradation pathway for UV treatment of amoxicillin (C = 25 mg L^{-1}, Pump speed = 10 rpm, and UV fluence rate = 4.86×10^{-6} Einstein $m^{-2} s^{-1}$).

of humic acid, no other byproduct formation was observed. In the presence of alkalinity, the pathway observed was the following: (a)–(c), or (d) and (e). When the system operated in the presence of both alkalinity and humic acid, the pathway observed was (a)–(c). Based on the observations, we can conclude that the elimination of amoxicillin molecules decreased in the presence of alkalinity and humic acid in the solution. Therefore, a lower byproduct formation was observed, while the rest was under the detection limit.

In contrast, the major byproduct profile difference between UV- and UV/H_2O_2-treated effluents is the observation of $[M]^+ = 429$ amu and $[M]^+ = 355$ amu mother ions when the system was operated with the UV/H_2O_2 process. $[M]^+ = 429$ amu is defined as *hydroxylated amoxicillin*, where hydroxyl radicals (OH·) were introduced into the amoxicillin molecule (1). In

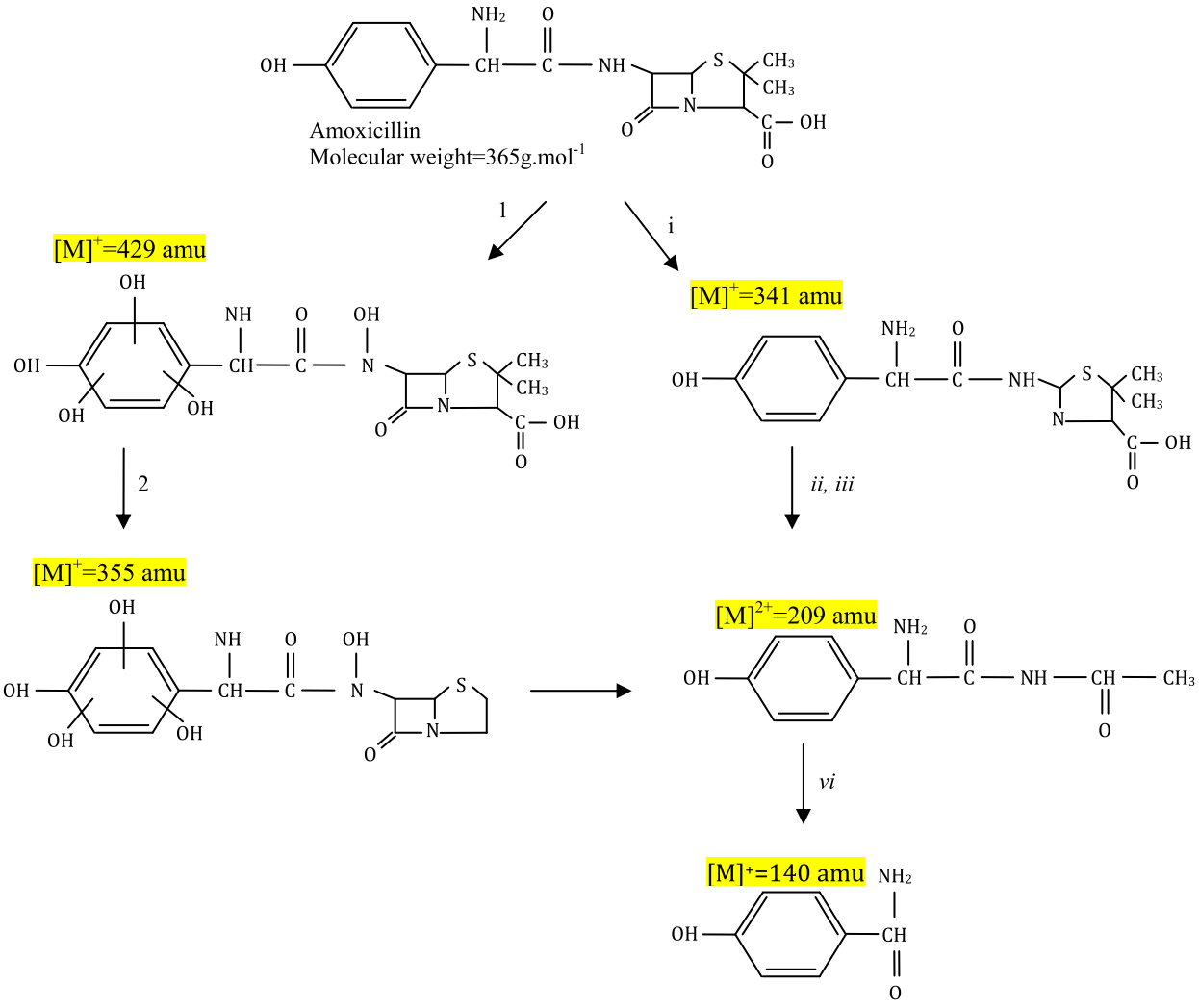

Fig. 9. Proposed degradation pathway for UV/H_2O_2 treatment of amoxicillin (C = 25 mg L^{-1}, Pump speed = 10 rpm, [H_2O_2] = 588 mg L^{-1}, and UV fluence rate = 4.86 × 10^{-6} Einstein m^{-2} s^{-1}).

addition, a $[M]^+$ = 355 amu ion was identified, and the proposed pathway suggests a decarboxylation (–COOH) and demethylation (–CH_3, –CH_3) of the $[M]^+$ = 429 amu ion (2). The remaining formation pathways were already observed and discussed with UV irradiation treatments. Under a matrix effect, no change was observed in the monitoring of byproducts due to the higher decomposition rate of amoxicillin molecules with UV/H_2O_2 than with UV irradiation alone. Therefore, the detection of byproducts after a UV/H_2O_2 process was achieved even in the presence of the matrix effects.

The UV spectrum of treated effluents also showed an increase in the absorbance of the 230 and 275 nm bands (Fig. 10), which indicates the formation of phenolic, anilinic, benzene, or quinone derivatives [42]. However, these distinct absorbance increases were not observed in the UV/H_2O_2-treated effluents due to the higher mineralization and lower amounts of observed phenolic, anilinic, benzene, or quinone derivatives.

3.5. Toxicity

The initial EC_{50}% value of the solutions prior to the experiments was 106.8%. After the UV treatment, this value decreased to 15.25% at a pump speed of 30 rpm (25.6 min residence time), which indicates the toxic nature of the effluents. Similarly, after the addition of alkalinity, humic acid, and both of them together, this value decreased to 13.35, 26, and 12.00%, respectively. After the UV/H_2O_2 treatment, the EC_{50}% values were 9.00%, which shows a more toxic nature after 25.6 min of treatment when the system operated

Table 3
Fragmentation of identified byproducts

Molecule	Fragment ions
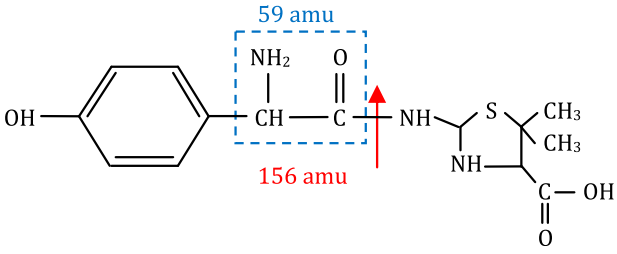	[M+] = 341 amu ($C_{15}H_{22}N_3O_4S$) Fragment ions = 156 amu ($C_7H_6O_3$) 59 amu (C_2H_5NO)
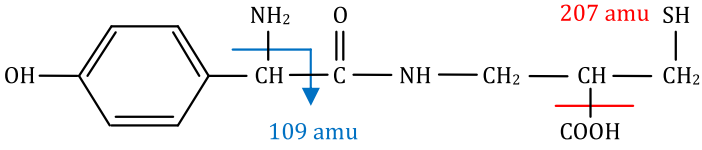	[M^{3+}] = 284 amu ($C_{12}H_{16}N_2O_4S$) Fragment ions = 207 amu ($C_{10}H_{11}N_2O_3$) 109 amu (C_7H_9O)
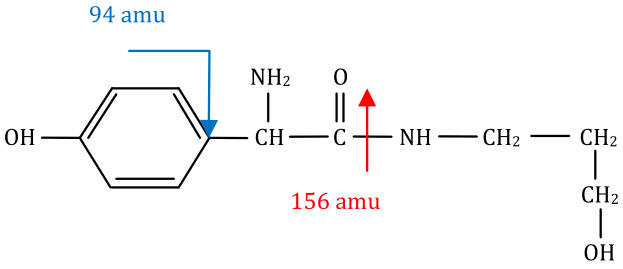	[M^{2+}] = 209 amu ($C_{10}H_{13}N_2O_3$) Fragment ions = 156 amu ($C_7H_6O_3$) 94 amu (C_6H_5OH)
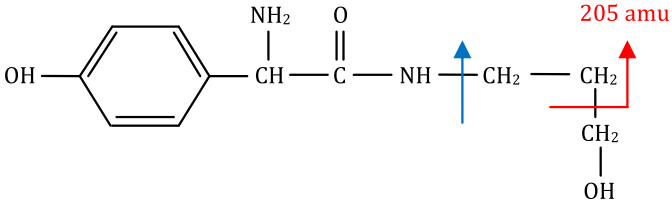	[M^{4+}] = 225 amu ($C_{11}H_{17}N_2O_3$) Fragment ions = 205 amu ($C_{10}H_9N_2O_3$) 177 amu
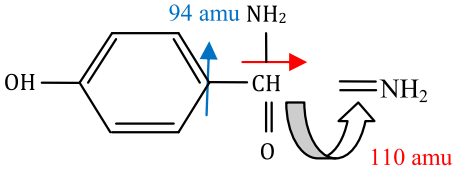	[M^{+}] = 140 amu ($C_7H_7O_3$) Fragment ion = 110 amu (C_6H_7NO) 94 amu (C_6H_5OH)
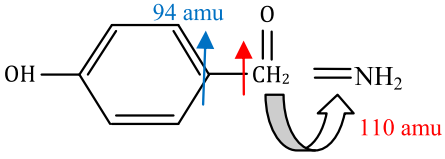	[M^{+3}] = 124 amu ($C_7H_8O_2$) Fragment ion = 110 amu (C_6H_7NO) 94 amu (C_6H_5OH)
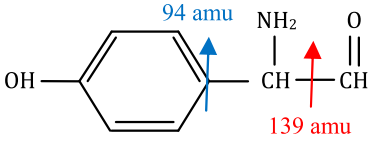	[M^{+6}] = 154 amu ($C_7H_8O_2$) Fragment ion = 139 amu ($C_7H_7O_3$) 94 amu (C_6H_5OH)

(*Continued*)

Table 3. (*Continued*)

Molecule	Fragment ions
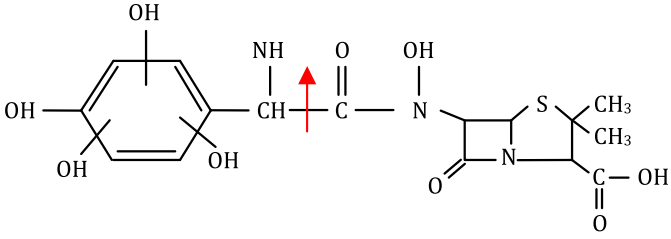	[M+] = 429 amu ($C_{16}H_{22}N_3O_9S$) Fragment ions = 124 amu ($C_7H_8O_2$)
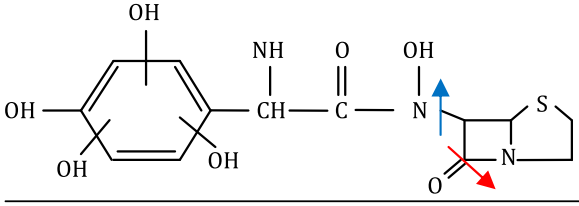	[M+] = 355 amu ($C_{13}H_{15}N_3O_7S$) Fragment ions = 341 amu ($C_{15}H_{22}N_3O_4S$) 249 amu ($C_8H_{12}N_2O_6$)

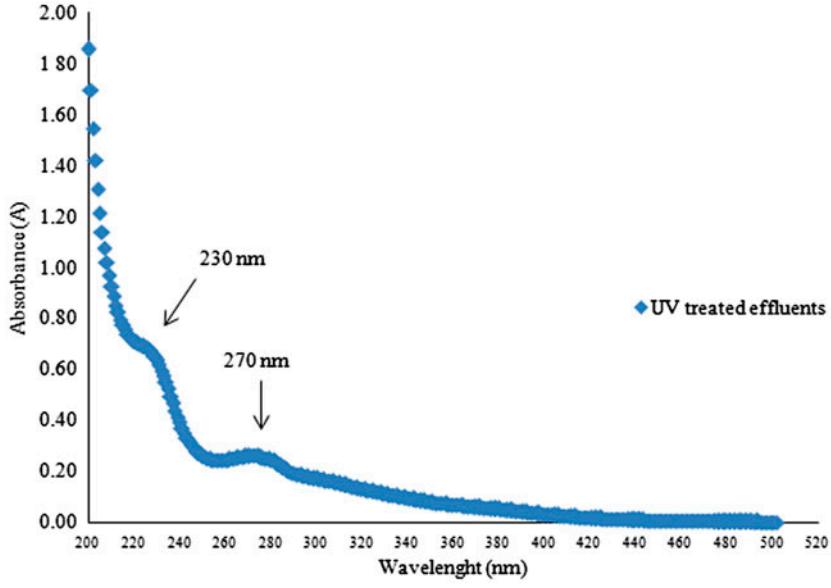

Fig. 10. UV spectrum of UV-treated samples (C = 25 mg L^{-1}, UV fluence rate = 4.86×10^{-6} Einstein m^{-2} s^{-1}. No obvious increase was observed after UV/H_2O_2 treatment due to higher mineralization).

at a pump speed of 30 rpm. In the presence of alkalinity, humic acid, and both of them together, the EC_{50}% value was 9.00, 12.00, and 10.00%, respectively.

When the system was operated for 67 min (10 rpm pump speed), the EC_{50}% value increased to 76.00 and 36.00% after the UV and UV/H_2O_2 processes, respectively. An increase in EC_{50}% indicates a less toxic nature of the treated effluents. The toxicity results are given in Table 4.

In the literature, the inhibition caused by amoxicillin on *Vibrio fischeri* micro-organisms (30%) showed

Table 4
EC_{50}% values after UV and UV/H_2O_2 treatment of amoxicillin solutions

Pump speed (rpm)	Residence time (min)	EC_{50}% UV	EC_{50}% UV/H_2O_2
Initial		*106.8*	
10	67.0	76	36

no significant change during the photo-Fenton process [15]. However, the monitored byproducts were limited, and the proposed byproduct formation pathway describes only the opening of the β-lactam ring and the thiazole ring. Conversely, the proposed byproduct pathway for UV-based oxidation of amoxicillin results in further rearrangements and cleavage of the molecule [29,30,42]. A survey in the literature [30], which was carried out using *E.coli* and *Bacillus subtilis*, indicates that the byproducts formed with the UV and UV/H_2O_2 oxidation also possess an antibacterial activity similar to the original compound (amoxicillin).

In this study, the initial EC_{50}% value of amoxicillin (106.8%) decreased to 76 and 36% after UV irradiation and a UV/H_2O_2 treatment due to the presence of identified byproducts. According to the Environmental Protection Agency database [10], amide-containing compounds pose a great toxicity risk to green algae micro-organisms compared to phenol, phenol amines, and carboxylic acids. Both of the studied processes mineralize the amoxicillin to byproducts that contain an amide functional group. However, due to the higher mineralization observed after the UV/H_2O_2 treatment, the presence of amide-containing byproducts, such as $[M]^+ = 140$, were expected to be higher, and they directly contribute to the toxicity of the sample. In addition, it was found that H_2O_2 itself has an EC_{50}% value of 14.36%, which can also be related to the higher toxicity found after the UV/H_2O_2 treatment of amoxicillin solutions.

4. Conclusion and recommendations

Plug flow reactors provide treatment options for larger volumes of aqueous solutions that contain target contaminants, and they are safer than a batch reactor type for the adjustment of UV lamps in the systems. In this study, 680 cm^3 volume aqueous solutions were treated with UV-based oxidation techniques. Interestingly, at the slowest pump speed conditions (10 rpm), which provide the longest residence time (67 min), 50 and 90% removal occurred after the UV and UV/H_2O_2 treatments, respectively. A number of adjustments can be made to the plug flow reactors to increase the removal efficiency and mineralization, such as changing the dimensions of the reactor and, therefore, the reactor volume; it is also possible to add more UV lamps, among other adjustments. In this study, the bench type of plug flow reactor resulted in nontoxic-treated effluents. Likewise, the proposed byproduct formation pathways were revealed. Matrix effects severely decrease the removal percentage and mineralization (approximately 50–70%) of the UV-based oxidation. Therefore, the use of this system in real wastewater treatment plants requires the consideration of these aspects before its application.

Acknowledgement

This doctoral thesis was supported by the Institute of Graduate Studies and Research, Cyprus International University. The authors thank the Instrumental Analysis Laboratory of Cyprus International University.

List of symbols

Φ (H^+)	—	quantum yield of H^+ formation
V_{tot}	—	total sample volume (cm^3)
M	—	surface area of the irradiated solution (cm^2)
$[H^+]$	—	hydrogen ion concentration (mol dm^{-3})
t	—	time (s)
N_L	—	Avogadro's number
I_{abs}	—	absorbed photon fluence rate
I_o	—	incident photon fluence rate
l	—	path length
ε	—	molar extinction coefficient (20 dm^3 mol^{-1} cm^{-1}) of potassium peroxodisulfate
c	—	concentration of potassium peroxodisulfate (0.01 M)
rpm	—	revolution per minute

References

[1] World Health Organization, (2012), Available from: <http:www.who.int/water_sanitation_health/publications/2012/pharmaceuticals/en/>. Accessed 20 March 2013.
[2] S. Börjesson, S. Melin, A. Matussek, P.E. Lindgren, A seasonal study of the mecA gene and *Staphylococcus aureus* including methicillin-resistant *S. aureus* in a municipal wastewater treatment plant, Water Res. 43 (4) (2009) 925–932.
[3] L. Rizzo, C. Manaia, C. Merlin, T. Schwartz, C. Dagot, M.C. Ploy, I. Michael, D. Fatta-Kassinos, Urban wastewater treatment plants as hotspots for antibiotic resistant bacteria and genes spread into the environment: A review, Sci. Total Environ. 447 (2013) 345–360.
[4] K. Kümmerer, Antibiotics in the aquatic environment—A review-Part I, Chemosphere 75 (2009) 417–434.
[5] T.A. Ternes, A. Joss, Human Pharmaceuticals, Hormones and Fragnences: The Challenge of Micropollutants in Urban Water Management, IWA Publishing, UK, 2006.
[6] A. Novo, S. André, P. Viana, O.C. Nunes, C.M. Manaia, Antibiotic resistance, antimicrobial residues and bacterial community composition in urban wastewater, Water Res. 47 (2013) 1875–1887.
[7] A. Lamm, I. Gozlan, A. Rotstein, D. Avisar, Detection of amoxicillin-diketopiperazine-2´,5´ in wastewater samples, J. Environ. Sci. Health., Part A 44 (2009) 1512–1517.

[8] I. Gozlan, A. Rotstein, D. Avisar, Amoxicillin degradation products formed under controlled environmental conditions: Identification and determination in the aquatic environment, Chemosphere 91 (2013) 985–992.
[9] A. Pérez-Parada, A. Agüera, M.M. Gómez-Ramos, J.F. García-Reyes, H. Heinzen, A.R. Fernández-Alba, Behavior of amoxicillin in waste water and river water: Identification of its main transformation products by liquid chromatography/electrospray quadrupole time-of-flight mass spectrometry, Rapid Commun. Mass Spectrom. 25 (2011) 731–742.
[10] Environmental Protection Agency, 2012, EPI SUITE™ Available from: <http://www.epa.gov/oppt/exposure/pubs/episuite.htm>. Accessed 12 December 2012.
[11] Environmental Protection Agency, 2013. Available from: <http://www.epa.gov/ppcp/>. Accessed 20 February 2013.
[12] J.A. Garrido, E. Brillas, P.L. Cabot, F. Centellas, C. Arias, R.M. Rodríguez, Mineralization of drugs in aqueous medium by advanced oxidation processes, Electrochim. Acta 25 (2007) 19–41.
[13] K. Ikehata, N.J. Jodeiri Naghashkar, M.G. Gamal El-Din, Degradation of aqueous pharmaceuticals by ozonation and advanced oxidation processes: A Review, Ozone Sci. Eng. 28 (2006) 353–414.
[14] V. Homem, A. Alves, L. Santos, Microwave-assisted Fenton's oxidation of amoxicillin, Chem. Eng. J. 220 (2013) 35–44.
[15] X. Li, T. Shen, D. Wang, X. Yue, X. Liu, Q. Yang, J. Cao, W. Zheng, G. Zeng, Photodegradation of amoxicillin by catalyzed Fe^{3+}/H_2O_2 process, J. Environ. Sci. 24(2) (2012) 269–275.
[16] A.G. Trovó, R.F. Pupo Nogueira, A. Agüera, A.R. Fernandez-Alba, S. Malato, Degradation of the antibiotic amoxicillin by photo-Fenton process—Chemical and toxicological assessment, Water Res. 45 (2011) 1394–1402.
[17] F. Ay, F. Kargi, Advanced oxidation of amoxicillin by Fenton's reagent treatment, J. Hazard. Mater. 179 (2010) 622–627.
[18] E.S. Elmolla, M. Chaudhuri, Degradation of the antibiotics amoxicillin, ampicillin and cloxacillin in aqueous solution by the photo-Fenton process, J. Hazard. Mater. 172 (2009) 1476–1481.
[19] E.S. Elmolla, M. Chaudhuri, Optimization of Fenton process for treatment of amoxicillin, ampicillin and cloxacillin antibiotics in aqueous solution, J. Hazard. Mater. 170 (2009) 666–672.
[20] A.G. Trovó, S.A.S. Melo, R.F.P. Nogueira, Photodegradation of the pharmaceuticals amoxicillin, bezafibrate and paracetamol by the photo-Fenton process—Application to sewage treatment plant effluent, J. Photochem. Photobiol., A 198 (2008) 215–220.
[21] V. Homem, A. Alves, L. Santos, Amoxicillin degradation at ppb levels by Fenton's oxidation using design of experiments, Sci. Total Environ. 408 (2010) 6272–6280.
[22] E.S. Elmolla, M. Chaudhuri, Improvement of biodegradability of synthetic amoxicillin wastewater by photo Fenton process, World Appl. Sci. J. 5(Special Issue for Environment) (2009) 53–58.
[23] E.S. Elmolla, M. Chaudhuri, Combined photo-Fenton-SBR process for antibiotic wastewater treatment, J. Hazard. Mater. 192 (2011) 1418–1426.
[24] R. Andreozzi, M. Canterino, R. Marotta, N. Paxeus, Antibiotic removal from wastewaters: The ozonation of amoxicillin, J. Hazard. Mater. 122 (2005) 243–250.
[25] F.J. Benitez, J.L. Acero, F.J. Real, G. Roldan, F. Casas, Comparison of different chemical oxidation treatments for the removal of selected pharmaceuticals in water matrices, Chem. Eng. J. 168 (2011) 1149–1156.
[26] F.J. Javier Benitez, J.L. Acero, F.J. Real, G. Roldán, Ozonation of pharmaceutical compounds: Rate constants and elimination in various water matrices, Chemosphere 77 (2009) 53–59.
[27] E.S. Elmolla, M. Chaudhuri, Photocatalytic degradation of amoxicillin, ampicillin and cloxacillin antibiotics in aqueous solution using UV/TiO_2 and UV/H_2O_2/TiO_2 photocatalysis, Desalination 252 (2010) 46–52.
[28] E.S. Elmolla, M. Chaudhuri, Degradation of amoxicillin, ampicillin and cloxacillin antibiotics in aqueous solution by the UV/ZnO photocatalytic process, J. Hazard. Mater. 173 (2010) 445–449.
[29] D. Klauson, J. Babkina, K. Stepanova, M. Krichevskaya, S. Preis, Aqueous photocatalytic oxidation of amoxicillin, Catal. Today 151 (2010) 39–45.
[30] Y.J. Jung, W.G. Kim, Y. Yoon, J. Kang, Y.M. Hong, H.W. Kim, Removal of amoxicillin by UV and UV/H_2O_2 processes, Sci. Total Environ. 420 (2012) 160–167.
[31] D. Dimitrakopoulou, I. Rethemiotaki, Z. Frontistis, N.P. Xekoukoulotakis, D. Venieri, D. Mantzavinos, Degradation, mineralization and antibiotic inactivation of amoxicillin by UV-A/TiO_2 photocatalysis, J. Environ. Manage. 98 (2012) 168–174.
[32] J.H.O.S. Pereira, A.C. Reis, O.C. Nunes, M.T. Borges, V.J.P. Vilar, R.A.R. Boaventura, Assessment of solar driven TiO_2-asissted photocatalysis efficiency on amoxicillin degradation, Environ. Sci. Pollut. Res. 21 (2013) 1292–1303.
[33] L. Rizzo, S. Meric, M. Guida, D. Kassinos, V. Belgiorno, Heterogenous photocatalytic degradation kinetics and detoxification of an urban wastewater treatment plant effluent contaminated with pharmaceuticals, Water Res. 43 (2009) 4070–4078.
[34] H.J. Kuhn, S.E. Braslavsky and R. Schmidt, Chemical Actinometry, International Union of Pure and Applied Chemisty, Division of Organic and Biomolecular Chemistry Sub-committee on Photochemistry, Technical Report, 2004.
[35] A. Rodrigues, A. Brito, P. Janknecht, M.F. Proença, R. Nogueira, Quantification of humic acids in surface water: Effects of divalent cations, pH, and filtration, J. Environ. Monit. 11 (2009) 377–382.
[36] R. Hofmann, R.C. Andrews, Impact of H_2O_2 and (bi)carbonate alkalinity on ammonia's inhibition of bromate formation, Water Res. 40 (2006) 3343–3348.
[37] O. Autin, J. Hart, P. Jarvis, J. MacAdam, S.A. Parsons, B. Jefferson, The impact of background organic matter and alkalinity on the degradation of the pesticide metaldehyde by two advanced oxidation processes: UV/H_2O_2 and UV/TiO_2, Water Res. 47 (2013) 2041–2049.
[38] D.D. Dionysiou, A.A. Cruz, M.I. Stefan, T. Kaloudis, T. Triantis, A. Hiskia, K.E. O'Shea, J.A. Westrick, M. Pelaez, X. He, Efficient removal of microcystin-LR

by UV-C/H_2O_2 in synthetic and natural water samples, Water Res. 46 (2012) 1501–1510.
[39] O. Autin, J. Hart, P. Jarvis, J. MacAdam, S.A. Parsons, B. Jefferson, Comparison of UV/TiO_2 and UV/H_2O_2 processes in an annular photoreactor for removal of micropollutants: Influence of water parameters on metaldehyde removal, quantum yields and energy consumption, Appl. Catal., B 138–139 (2013) 268–275.
[40] N.C. Sawyer, P.L. McCarty, G.F. Parkin, Chemistry for Environmental Engineering and Science, fifth ed., McGraw-Hill, New York, NY, 2003.
[41] M. Magureanu, D. Piroi, N.B. Mandache, V. David, A. Medvedovici, C. Bradu, V.I. Parvulescu, Degradation of antibiotics in water by non-thermal plasma treatment, Water Res. 45 (2011) 3407–3416.
[42] A. Ziylan, S. Dogan, S. Agopcan, R. Kidak, V. Aviyente, N. Ince, Sonochemical degradation of diclofenac: Byproduct assessment, reaction mechanisms and environmental considerations, Environ. Sci. Pollut. Res. 21(9) (2014) 5929–5939.